Journal of Mines, Metals and Fuels, 71(12B) : 21-26; 2023. DOI: 10.18311/jmmf/2023/45493

Print ISSN : 0022-2755

Journal of Mines, Metals and Fuels

Contents available at: www.informaticsjournals.com/index.php/jmmf

The High Strain Rate Response of A Bio-Mimetic Composite Plates

Pankaj Gupta[1] **and Yogesh Shrivastava**[2*]

[1]*Jaypee University of Engineering and Technology, Raghogarh, Guna – 473226, Madhya Pradesh, India*
[2]*Galgotias College of Engineering and Technology, Greater Noida – 201310, Uttar Pradesh, India; yogeshshrivastava90@gmail.com*

Abstract

Biological materials are often viewed as composites, consisting of weaker components arranged hierarchically, leading to exceptional mechanical capabilities that are challenging to replicate in synthetic materials. Natural shape and structure develop through the process of striving for improved performance. This paper will provide a summary of observations from experiments conducted on a composite material designed to closely mimic a sophisticated multifunctional biological structure. The Split Hopkinson Pressure Bar (SHPB) was utilized to test strain rates ranging from 10^2 s^{-1} to 10^4 s^{-1}, providing reliable and comprehensible data for analyzing the behavior of the composite material at high strain rates. The Split Hopkinson Pressure Bar (SHPB) device is frequently utilized for evaluating metals and other materials with high strength and mechanical resistance. This study will detail the changes made to a standard Split Hopkinson Pressure Bar (SHPB) apparatus for testing low impedance materials. An aluminum sample was seen to lose its specific stiffness as impact strain rate increased, but the produced material continued to improve.

Keywords: *Composite, Strain Rate, Split Hopkinson Pressure Bar*

1.0 Introduction

Biological materials are typically viewed as composites composed of rather fragile components. Their hierarchical structure leads to a unique mix of mechanical qualities like as stiffness, strength, toughness, and low density, which are challenging to achieve in synthetic materials[1]. Researchers have recently become interested in studying these materials, specifically focusing on their structure-property relationship. There is a growing interest in the materials research community to comprehend the mechanisms that control the behavior of natural materials in order to replicate them in newly created synthetic materials[2]. The field of study known as biomimetics has resulted in numerous advancements in material science. It is a multidisciplinary study subject that has lately been applied in several technical contexts. Biomimetics is a design methodology that involves creating novel materials and addressing technical challenges by imitating natural structures. Nature contains numerous sophisticated systems that can be readily replicated using modern technologies[3]. Over the past few decades, the biomimetic approach has resulted in a wide range of solutions inspired by nature, also referred to as bio-inspired or biomimetic structures[4,5].

Wood, bone, and nacre are regarded intriguing structural materials among biological composites due to their load-bearing capabilities. These materials are now being viewed as biomimetic models, leading to the creation of new biomimetic solutions. Bone is highly valued for its

**Author for correspondence*

superior mechanical qualities, such as stiffness, strength, and toughness, which make it an excellent support structure for many species[6,7]. Bone is a highly old and prevalent biological material that has been extensively studied for many years. It serves as a significant source of inspiration for various biomimetic materials[8-10]. Bone's distinct mechanical characteristics, including stiffness, strength, and toughness, make it an appealing biomimetic model for research and development of newly created biologically inspired composites. Bone is a mineral-protein combination noted for its exceptional toughness. This mechanical property is significantly higher, by three to five orders of magnitude, than that of its basic mineral due to toughening mechanisms at several hierarchical levels[11].

This study examines the response of a sandwiched composite material at high strain rates, which is engineered to replicate the structure of human skull bones[12,13]. The composite consists of a low impedance foam core layer shielded by high strength fiber reinforced skin layers[11,14]. This study aims to investigate if the split Hopkinson Pressure Bar (SHPB) equipment can provide reliable and comprehensible data for analyzing low impedance materials under high strain rates. This device is frequently utilized to test metals and other materials with high strength and mechanical impedance. Engineering materials like rubbers and foams are being employed more frequently in applications that involve high strain rates and deformations.

2.0 Methodology

This section outlines the biomimetic method employed to replicate the microstructure of biological structure in a new composite material, covering the entire process from the initial idea to the final product design and production. The method used to replicate the internal structure of biological structure involves several phases: selecting the hierarchical level to imitate specific toughening mechanisms, defining a concept, assessing feasibility, choosing materials and manufacturing techniques, and finally, the implementation. In addition to the bio-inspired composite, we also provide the design and characterization of a traditional laminate with a similar kind and quantity of reinforcement and matrix as the bio-inspired composite, but with a different internal structure. The bio-inspired composite material design is not intended to simply replicate the microstructure of biological structure. The structure is simplified and contains the major characteristics involved in the fracture process, such as osteons, which are replicated on a bigger scale using synthetic fibers. We want to imitate bone structure to reproduce the primary toughening mechanisms that take place in bone at this hierarchical level.

At high speeds, even lightweight items can produce a considerable amount of impact energy, which can negatively damage the performance and durability of the constructed component when the energy is transferred through it. Developing enhanced lightweight composite materials that can reduce the transmission of impact energy is advantageous for several applications. Testing polymer materials with a SHBP system can be challenging because of their low mechanical impedance. The mechanical impedance, denoted as 'Z', is calculated by multiplying the area, density, and longitudinal sound speed. To achieve maximum sensitivity from the instrument, it is ideal to closely match the impedance of the pressure bar material to that of the sample. Table 1 presents the Mechanical Impedance values for specific metals and polymers. The multi-layer polymer composite effectively reduces the compressive strain-waves generated by the initial impact, making it challenging to obtain accurate readings from the strain gage on the output bar of the SHPB system. Using a high initial impact velocity is preferred since it results in a larger amplitude wave, making it easier to measure precisely. The highest impact velocity that can be utilized is restricted by the material qualities of the pressure bars. To prevent damage to the bars, the impact

Table 1. Impedance of various materials

Metals and Alloys	Impedance
304 Stainless Steel	36.08
Brass	31.48
Titanium	23.64
Beryllium	14.80
6061 Aluminum	14.40
AZ31B Magnesium	8.02
Polymers	**Impedance**
Neoprene	4.01
Teflon	3.96
Polyurethane	3.14
Nylon	2.93
Lucite	2.67

pressure should not exceed the Yield Strength of the bar material. The impact pressure is calculated by the Rankine-Hugoniot Jump Equations, which depend on the density, sound speed, and impact velocity. Table 2 displays the maximum permitted impact velocities for Aluminum 6061 and Magnesium AZ31B alloy pressure bars, based on yield strengths of 145 MPa and 97 MPa for the corresponding alloys. The Magnesium AZ31B alloy enables a 20% increase in wave amplitude compared to the previously employed Aluminum 6061 bars.

2.1 Split Hopkinson Pressure Bar (SHPB)

The equipment consists of a gas pistol with an impactor bar, an input bar, and an output bar. A shock wave is sent by the impactor through the input bar, the sample being studied, and the output bar. Figures 1 illustrate the setup of the device. A strain gauge measures the strain caused by the shockwave in the input and output bars. This information is then used to figure out the material's strain and other features. Figure 2 illustrates the diagram showing the links between the sample and the input and output bars. As Kaiser[1] says, the SHPB ideas can be summed up like this:

1. The relationship between strain rate and stress is the amount of waves that are reflected and transmitted.
2. By integrating the test's strain rate trend over time, the strain in the sample may be found.
3. You may determine the stress-strain features by looking at the strain in the input and output bars. The form of the impact is illustrated in Figure 3.

The impactor hits the input bar (incident bar), which makes a pulse that is measured by the strain gauge on the incident bar. The input bar and sample interface then send back a pulse that is measured by the strain gauge in the incident bar. The strain gauge on the impact bar measures both the pulse that comes in εi (t) and the pulse that bounces back εr (t). Ninan *et al.*[2] shows the detail mathematical functionality of SHPB illustrated in Figure 3.

Table 2. Maximum impact velocities required to remain below bar yield point

Bar Material	Maximum Velocity (m/s)	Maximum Velocity (MPH)
6061 Aluminum	20.0	44.74
AZ31B Magnesium	24.1	53.91

Composites can also be calculated using the Split Hopkinson pressure bar formula that was stated earlier. According to Ninan *et al.*[2], statistically characterizing the rate-dependent deformation of composite laminates outside of the elastic domain has only been attempted a handful of times, and that was just recently. Figure 4 displays the loads, displacements, and stresses at different places on the sample.

An elastic wave is produced by the impactor's collision with the incident bar and propagates through the specimen and bars. The specimen undergoes plastic deformation as a result of the elastic wave. Research involving plastic wave propagation is not appropriate for the SHPB. When testing low impedance materials for high strain rate characteristics, the SHPB can be useful. Since the majority of the incident pulse is reflected back into the incident bar and only a small amount is transmitted to the transmission bar, low-impedance materials enable the incident bar-specimen interface to move freely under stress wave loading. The incident bar should be made of high-strength aluminum alloy, while the transmission bar should be constructed from a hollow aluminum tube. As per Equation 9, the presence of the hollow aluminum tube will lead to a rise in σs stress. In the transmission bar, the signal will be amplified by means of the hollow tube. A circular piezoelectric transducer, which is essentially an X-cut quartz crystal disk, can be inserted into the center of an aluminum transmission bar of matching diameter to directly measure the time-resolved transmitted force. This

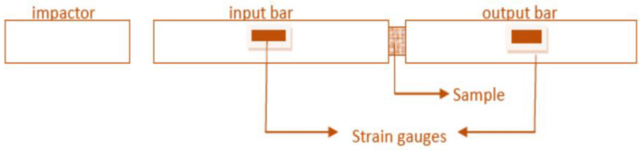

Figure 1. Schematic illustration of the SHPB setup.

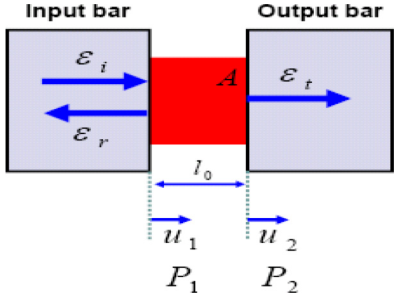

Figure 2. Sample-bar interface and sample.

εi (t) and εr (t) measure how far the incident bar-sample interface moves, which is denoted by uI (t).

$$\varepsilon i(t) = \varepsilon I(t - \Delta t) \qquad (1)$$

$$\varepsilon r(t) = \varepsilon I(t + \Delta t) \qquad (2)$$

The pulse takes Δt time to get from the strain gauge on the input bar to the sample, and t is a single instant in time.

$$u1 = C0 \int_0^t (-\varepsilon_i + \varepsilon_r)\, dt \qquad (3)$$

In equation 3, the distance between the input bar and the sample interface is shown. In equation 4, the distance between the sample bar and the output bar is shown.

$$u2 = -C0 \int_0^t \varepsilon_t\, dt \qquad (4)$$

The average strain in the sample is:

$$\varepsilon s = \frac{u_2 - u_1}{l_0} = \frac{C_0}{l_0} \int_0^t (-\varepsilon_t + \varepsilon_i - \varepsilon_r) dt \qquad (5)$$

l0 is the sample length and C0 is the longitudinal wave velocity in the bar. Loads at the sample interfaces P1 and P2 can be determined from the folowing equations:

$$P1 = AsE\, (\varepsilon i + \varepsilon r) \qquad (6)$$

$$P2 = AsE\varepsilon t \qquad (7)$$

Assuming that the pressure difference at each interface of the sample is negligibly small then according to Graff 3, εt = εi + εr and substituting this into equation 5 gives:

$$\varepsilon s(t) = -\frac{2C_0}{l_0} \int_0^t \varepsilon_r dt \qquad (8)$$

which represents the sample average strain. The stress is obtained directly from the transmitted strain, and the strain rate in the speciment from the reflected strain and are given by;

$$\sigma s = E\frac{A_0}{A_s}\varepsilon t \qquad (9)$$

$$\dot{\varepsilon} s = \frac{-2C_0}{l_0}\varepsilon r \qquad (10)$$

Figure 3. Ninan *et al.*[2] shows the mathematical functionality of SHPB.

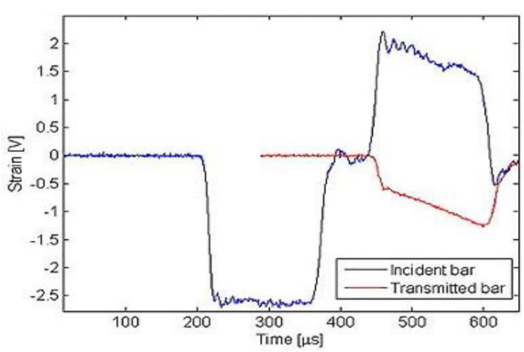

Figure 4. Shape of incident, reflected and transmitted pulse.

improves the signal in the bar, which is useful for testing low-impedance materials. When it comes to sensing forces in the x-direction, X-cut quartz outperforms the indirect surface strain gage method. The self-generating quartz transducer's mechanical impedance is nearly identical to the aluminum transmission bar's mechanical impedance, therefore adding the quartz disk won't affect the bar's ability to transmit waves in a single dimension.

3.0 Results and Discussion

Plates measuring 10.16 cm by 10.16 cm from Table 1 were utilized to assess the physical properties. Test samples with a diameter of 25.4 mm were cut from the plates. Figure 5 displays test observations for two samples (Blue curve for 779 Kevlar on both sides and red curve for Aluminum). The plots illustrate the relationship between specific stiffness, which is defined as the ratio of stiffness (in MPa) to mass density (in N/m^3), and strain rate (per second). To compare the observation of the created composite, an isotropic material like as Aluminum is used. The red curve shows how specific stiffness changes with strain rate for aluminum, whereas the blue curve represents the specific stiffness variation for the composite with two skin layers on either side of the core layer. To investigate the impact behavior of a composite material with a foam core and FRP skin layers on both sides, the standard Split Hopkinson Pressure Bar (SHPB) apparatus was modified. The transmitted pulse's signal is amplified using an

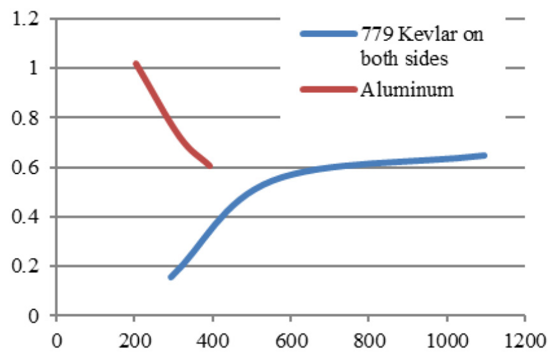

Figure 5. Specific stiffness with strain rate.

aluminum tube with an empty space within serving as the output bar. A small amount of signal is passed through the specimen because the low impedance of the foam material causes the incidence pulse to bounce back into the incident bar.

4.0 Conclusions

Because its internal structure is different, the mechanical behavior of the newly created biomimetic composite differed from that of the conventional one. The bio-inspired construction exhibits enhanced characteristics and, as anticipated, a notable anisotropy. To verify that the low impedance material mainly causes most of the incident wave to bounce back into the input bar, an aluminum disc specimen is tested on the Split Hopkinson Pressure Bar (SHPB). Results from the aluminum disc test show that the response from the output bar represents the majority of the incoming pulse that goes through the sample. According to equation 9, the transmitted pulse determines the impact-induced tension in the sample. Since the input and output bars show the intensity of the impact load immediately, testing proves that larger impact loads cause increased stress on the aluminum sample. A decrease in modulus is observed as the strain rate of the aluminum sample is increased. As the strain rate increases, the samples of the produced composite become stiffer. At first, the aluminum sample's cross-section is not deformed as much because of its higher modulus of elasticity. As strain increases, the material stiffens up as a result of work-hardening that occurs during deformation. Composite specimens exhibit a rise in modulus with increasing strain rate. There is room for improvement in the proposed design. By including nanoparticles that serve as reinforcements, ideally with a platelet shape and appropriate size characteristics, as indicated by the outcomes of molecular dynamics simulations.

5.0 References

1. Kaiser MA. Advancements in the split Hopkinson bar test [dissertation]. Virginia Tech.
2. Ninan L, Tsai J, Sun CT. Use of split Hopkinson pressure bar for testing off-axis composites. Int J Impact Eng. 2001; 25(3):291-313. https://doi.org/10.1016/S0734-743X(00)00039-7
3. Graff KF. Wave motion in elastic solids. Courier Corporation; 2012.
4. Van Le T, Ghazlan A, Ngo T, Nguyen T, Remennikov A. A comprehensive review of selected biological armor systems-from structure-function to bio-mimetic techniques. Comp Struct. 2019; 225:111172. https://doi.org/10.1016/j.compstruct.2019.111172
5. Kim DK, Kim HI, Han JH, Kwon KJ. Experimental investigation on the aerodynamic characteristics of a bio-mimetic flapping wing with macro-fiber composites. J Intell Mat Syst Struct. 2008; 19(3):423-31. https://doi.org/10.1177/1045389X07083618
6. Shavandi A, Bekhit AE, Ali MA, Sun Z. Bio-mimetic composite scaffold from mussel shells, squid pen and crab chitosan for bone tissue engineering. Int J Biol Macromolecul. 2015; 80:445-54. https://doi.org/10.1016/j.ijbiomac.2015.07.012 PMid:26187191
7. Park JH, Yoon KJ, Park HC. Development of bio-mimetic composite wing structures and experimental study on flapping characteristics. 2007 IEEE Int Conf Rob Biomimet (ROBIO); 2007. p. 25-30.
8. Libonati F, Colombo C, Vergani L. Design and characterization of a biomimetic composite inspired to human bone. Fatig Fract Eng Mat Struct. 2014; 37(7):772-81. https://doi.org/10.1111/ffe.12172
9. Libonati F. Bio-inspired Composites: Using nature to tackle composite limitations. Adv Eng Mat Model. 2016:165-90. https://doi.org/10.1002/9781119242567.ch5
10. Ganjali H, Ganjali MR, Alizadeh T, Faridbod F, Norouzi P. Bio-mimetic cadmium ion imprinted polymer based potentiometric nano-composite sensor. Int J Elect Sci. 2011; 6(12):6085-93. https://doi.org/10.1016/S1452-3981(23)19664-7
11. Tang D, Zhang L, Zhang X, Xu L, Li K, Zhang A. Bio-mimetic actuators of a photothermal-responsive vitrimer liquid crystal elastomer with robust, self-healing, shape memory, and reconfigurable properties. ACS Appl Mat Interf. 2021; 14(1):1929-39. https://doi.org/10.1021/acsami.1c19595 PMid:34964343
12. Kumar M, Jha AK, Bhagoria Y, Gupta P. A review to explore different meshless methods in various Structural prob-

lems. IOP Conf Series: Mat Sci Eng. 2021; 1116(1):012119. https://doi.org/10.1088/1757-899X/1116/1/012119

13. Maithil P, Gupta P, Chandravanshi ML. Study of mechanical properties of the natural-synthetic fiber reinforced polymer matrix composite. Mat Today: Proc. 2023. https://doi.org/10.1016/j.matpr.2023.01.245
14. Jianxun D, Chengzhou X, Zhengjian F, Chaoqi X, Kai L. Numerical investigation on energy absorption characteristics of impact-resistant lightweight structure of bio-mimetic micro aerial vehicle. Proc Institut Mech Eng, Part L: J Mat: Design Appl. 2023:14644207231217032. https://doi.org/10.1177/14644207231217032